

Cell Fusion and Intramembrane Particle Distribution in Polyethylene Glycol-resistant Cells

DAVID S. ROOS, JOHN M. ROBINSON, and RICHARD L. DAVIDSON

The Rockefeller University, New York 10021; and Departments of Pathology and Microbiology and Molecular Genetics, and the Division of Human Genetics, Children's Hospital Medical Center, Harvard Medical School, Boston, Massachusetts 02115. Dr. Davidson's present address is Center for Genetics, University of Illinois College of Medicine, Chicago, Illinois 60612.

ABSTRACT The distribution of intramembrane particles (IMP) as revealed by freeze-fracture electron microscopy has been analyzed following treatment of mouse L cells and fusion-deficient L cell derivatives with several concentrations of polyethylene glycol (PEG). In cell cultures treated with concentrations of PEG below the critical level for fusion, no aggregation of IMP was observed. When confluent cultures of the parental cells are treated with 50% PEG, >90% of the cells fuse, and cold-induced IMP aggregation is extensive. In contrast, identical treatment of fusion-deficient cell lines shows neither extensive fusion nor IMP redistribution. At higher concentrations of PEG, however, the PEG-resistant cells fuse extensively and IMP aggregation is evident. Thus the decreased ability of the fusion-deficient cells to fuse after treatment with PEG is correlated with the failure of IMP aggregation to occur.

A technique for quantifying particle distribution was developed that is practical for the accurate analysis of a large number of micrographs. The variance from the mean number of particles in randomly chosen areas of fixed size was calculated for each cell line at each concentration of PEG. Statistical analysis confirms visual observation of highly aggregated IMP, and allows detection of low levels of aggregation in parental cells that were less extensively fused by exposure to lower concentrations of PEG. When low levels of fusion were induced in fusion-deficient cells, however, no IMP aggregation could be detected.

The fusion of biological membranes is an integral component of many physiological phenomena. Membrane fusion is found in all taxonomic kingdoms and at various levels of cellular organization. In animal systems, fusion is known to occur at the multicellular level during tissue differentiation, and in the pathogenesis of certain tumors and viral infections. Cell membranes undergo fusion in the course of mitosis, and in such specialized events as sperm-egg fusion during fertilization and the formation of macrophage giant cells during certain types of immune response. Fusion is a necessary event in any cellular activity involving vesiculation, including endocytosis, exocytosis, and compartmentalized intracellular transport. For reviews on membrane fusion, see reference 48.

A number of techniques are available that induce fusion in natural and artificial systems. Various chemical treatments (2, 13, 28, 30, 56), lipid vesicles (41), ionic manipulations (11, 42), and virus particles (25, 26, 39) have been reported to cause fusion in certain experimental situations. Applications of membrane fusion are currently in use or under develop-

ment, including the production of hybridomas (17) and the controlled distribution of material to cell populations (41), especially as a route for tumor chemotherapy (3). The ability to control cell fusion has also opened up broad areas of somatic cell science for analytical investigation (12). Studies in genetics have primarily used Sendai virus (24) and, more recently, polyethylene glycol (PEG;¹ 13, 49) to induce hybrid formation. PEG-induced fusion is inexpensive, reproducible and highly controllable, and does not require the addition of extraneous biological material.

Several morphological studies of both naturally occurring and induced membrane fusion have been made, but the specific biochemical mechanisms involved are still unknown.

¹ *Abbreviations used in this paper:* IMP, Intramembrane particles; LM, 5-bromodeoxyuridine-resistant mouse fibroblast cell line LM(TK⁻) Clone 1D; PEG, polyethylene glycol; E medium, Dulbecco's modified Eagle's medium; E+S, E medium supplemented with 10% fetal calf serum.

Common features associated with cell fusion include cell aggregation, swelling, and/or lysis (2, 32, 50, 60). At the level of electron microscopic analysis, the appearance of pentalamellar membrane structures and redistribution of intramembrane particles (IMP) have been reported (5, 29, 31, 50, 58).

We recently succeeded in isolating, from a highly fusible parental stock, a series of homogeneous, stable cell lines which are increasingly resistant to the fusogenic effects of PEG (51). The least fusible of these cells exhibit <20% fusion under the same conditions that induce >90% fusion in the parental line. At higher concentrations of PEG, resistance to fusion can be overcome. This system provides the advantage of closely related cell lines that differ only as the result of strong selection for decreased fusion following a standard PEG treatment. We have initiated a systematic study of the fusible cell line LM and its fusion-deficient derivatives, and here present evidence that resistance to fusion by PEG in these cells is correlated with a resistance to cold-induced aggregation of IMPs following PEG treatment.

MATERIALS AND METHODS

Cells and Media: The parental cell line used in this study was the 5-bromodeoxyuridine-resistant mouse fibroblast cell line LM(TK⁻) Clone 1D (referred to as LM). The isolation of PEG-resistant cell lines has been reported previously (51). Briefly, cultures were treated with PEG (in the same manner as described below) and cells which remained unfused were allowed to proliferate. Repeated cycles of selection generated increasingly resistant cell lines, referred to as F₈, F₁₆, F₂₄, etc., where the subscript refers to the number of cycles of selection which these cells have survived.

All cells were grown in Dulbecco's modified Eagle's medium (referred to as E medium) supplemented with 10% fetal calf serum (E+S medium). The cultures were incubated at 36.5°C in an atmosphere of 7% CO₂. Cultures were maintained and treated in Falcon plastic tissue culture ware (Falcon Labware, Oxnard, CA).

Fusion Protocol: Cells were collected by trypsinization from dense cultures in 75-cm² flasks and inoculated into either 60-mm or 35-mm diameter petri dishes containing glass coverslips. The 60-mm and 35-mm dishes were inoculated with 4×10^6 cells in 5 ml E+S medium or 1.5×10^6 cells in 3 ml of medium, respectively. All cultures were incubated overnight prior to fusion. These preparations yield homogenous confluent monolayers of cells.

Fusion of cells on coverslips followed the procedure described previously (50). Coverslips were transferred to a fresh 35-mm petri dish and covered with 3 ml of warm PEG solution (J.T. Baker Chemical Co., Phillipsburg, NJ; PEG 1000 diluted (wt/vol) in E medium to various concentrations as described in the text. Following 1-min incubation in the PEG solution, coverslips were removed with forceps and rinsed by repeated dipping in a large volume of E medium. The coverslips were then transferred to fresh petri dishes and incubated for various times in E+S medium.

Cultures in 60-mm dishes were fused as described by Roos and Davison (51). Culture medium was aspirated and replaced with 3-ml PEG solution. After treatment for 1 min, the PEG was rapidly aspirated and the monolayer rinsed with five 10-ml washes of fresh E+S medium in quick succession.

The times of fusion referred to in this paper indicate the period between removal from the PEG solution and fixation, trypsinization or preparation for freeze-fracture. In all experiments, control cultures were treated in parallel with E medium substituted for the PEG solution.

Light Microscopy: Cells were grown on 18 mm² #1 glass coverslips (Fisher Scientific Co., Pittsburgh, PA) in 35-mm petri dishes. After treatment with PEG and fusion for 90 min, coverslips were fixed for 5 min in methanol, stained in Giemsa's (Fisher Scientific Co.), and mounted in Uvinert Aqueous Mountant (Searle Diagnostics, Oakville, Ontario, Canada). Cultures were observed under a Zeiss Photomicroscope III equipped with phase-contrast optics. Observations were recorded on 35mm Ilford Pan F film (ASA 50).

Quantification of Fusion: Fusion was quantified as described previously (51). Cells grown in 60-mm dishes were fused and incubated for 90 min, by which time fusion was virtually complete. Cells were then collected by trypsinization and replated into at least three 60-mm dishes, each receiving one-tenth of the treated sample. After sufficient incubation to allow cell attachment, dishes were rinsed in saline solution, fixed in methanol, and stained in Giemsa's. The extent of fusion was quantified as "percent fusion," defined as the number of nuclei in fused cells divided by the total number of nuclei

present, times 100. At least 1,000 nuclei were counted per sample.

Freeze-Fracture: Cell cultures were inoculated into 35-mm dishes containing several 4-mm diameter #0 glass coverslips attached to larger coverslips for ease in handling. After fusion and incubation, coverslip assemblies were dipped once in E medium and once in 0.1 M cacodylate buffer (pH 7.4) at room temperature and held in cacodylate buffer at 4°C for 10 min. The buffer was then replaced with 3% glutaraldehyde in 0.1 M cacodylate. Cells were fixed at 4°C for 30 min and then allowed to return to room temperature for an additional 30 min of fixation. After fixation, the coverslip assemblies were washed several times with buffer and the small coverslips were transferred to 30% glycerol in 0.1 M cacodylate buffer for ~12 h. The larger support coverslips were stained with Giemsa's for visual assessment of fusion.

The 4-mm coverslips were processed according to the monolayer fracture technique of Yee et al. (62). For this procedure, the small coverslips were mounted on gold-plated specimen carriers, frozen as a unit in Freon 22, and transferred to a Balzers double-replica device (Balzers, Hudson, NH). The assembly was then broken apart in a Balzers BA 360M freeze-cleave apparatus at -150°C, and the fractured sample shadowed with platinum and coated with carbon. The replica was teased away from the gold specimen support in distilled water, and the glass coverslip was removed from the complementary replica in hydrofluoric acid. After digestion of all biological material with 5% hypochlorite (Clorox bleach) and dimethylformamide, replicas were supported on formvar-coated grids and examined in a Philips 200 electron microscope under an accelerating voltage of 60 kV. All freeze-fracture micrographs presented in this report are of the P fracture face, according to the nomenclature of Branton et al. (8).

Quantification of IMP Distribution: Fractures of individual cells or of portions of syncytia were located on electron microscope grids at low magnification, where detailed morphology of the fractured face could not be resolved. Magnification was then increased without further selection of field. Micrographs were taken at an initial magnification of 19,000, and then enlarged to a final magnification of 46,500.

An acetate overlay was marked at locations generated randomly by computer with 15 sequentially numbered squares of 4 mm on a side (termed quadrats). Each photograph was aligned underneath the acetate sheet and the number of IMP in each of the first 10 numbered quadrats was scored. In cases where a quadrat revealed a distorted membrane surface or no membrane at all (due to folding or wrinkling of the replica, a tear in the formvar coating, a fracture plane through the cytoplasm, etc.) additional numbered squares were scored until a total of 10 areas had been counted. It was never necessary to examine more than 15 quadrats to find 10 that were usable. At least four cells were photographed from each experiment. When experiments were combined, a total of at least ten cells were analyzed for each treatment. Micrographs were mixed together and randomly selected for analysis of IMP distribution. The individual who counted IMP was not aware of which sample was being counted.

Statistics: For each cell analyzed, the variance from the mean number of IMP per quadrat was calculated (V , defined as $[\text{standard deviation}]^2/\text{mean}$), and plotted in relation to $V = 1$, as predicted from the Poisson distribution for a randomly distributed sample. Measurements of $V < 1$ indicate nonrandom distribution in the form of a regular pattern, while measurements of $V > 1$ indicate nonrandom distribution in the form of clumped, or aggregated, IMP. The calculation of V as a function of the mean allows comparison between cells that differ in overall IMP density. This form of analysis has previously been applied to both one- (46) and two- (16, 61) dimensional systems.

Confidence limits for experimental measurements of V were calculated by the jackknife technique (so named because of its versatility; 37, 38). The jackknife statistic provides an internal analysis of variability by comparing V 's calculated when one data point is omitted. The 99% confidence levels were derived by transformation of values of V to a symmetric distribution ($\log V$) and calculation from tables of critical values for the Student's t -evaluation as described by Singer et al. (54).

We also compared Poisson expectations directly with the frequency distribution of quadrats containing different numbers of IMP. Deviation from the predicted curve was evaluated by the Chi-square test. For this evaluation, quadrat counts from all photographs of identically treated samples were pooled, and the Chi-square value was calculated for the different densities of IMP per quadrat (1, 36, 43). These values were totaled to provide a cumulative Chi-square value which reflects the difference between observed and Poisson distributions. The tails at each end of the distributions were pooled so that no channel had an expected frequency of less than one quadrat. Nonrandom distributions were classified as statistically significant at P values <0.01.

RESULTS

Fusion of Parental and Resistant Cells

We have previously reported the formation of extensive

syncytia in LM cells treated with 50% PEG (13, 15, 50). Further work from this laboratory has described the isolation (by repeated cycles of PEG treatment) of a series of cell lines that are increasingly resistant to the fusion inducing effects of PEG (51). Fig. 1 demonstrates the decreased fusion associated with treatment of these lines with 50% PEG as described in Materials and Methods. Fewer than 10% of all cells in LM cultures remained as mononucleates following PEG treatment. In seven separate fusions of the parental LM line the percentage of cells which fused varied from 83% to 99% (average 93%, standard deviation 5.7%).

Cell lines F_{32} and F_{40} are recent isolates, selected subsequent to our initial report. While F_{32} cells show significantly increased resistance to PEG-induced fusion relative to the F_{24} line, the difference in fusion response between F_{32} and F_{40} cannot be distinguished from that between fusion of a given line in two different experiments. It thus appears that we have reached the limit of selection for fusion resistance achievable by this technique.

The dependence of fusion on PEG concentration (7, 15, 60) is presented photographically in Fig. 2 and graphically in Fig. 3. When treated with 30% PEG, LM cells are not induced to fuse above control levels. Treatment of LM cells with 40% PEG induces ~50% of cells to form multinucleates, while either 50% or 55% PEG treatment of LM cells induces >90% fusion.

The sharp rise in fusibility of LM cells within this narrow range of PEG concentration suggested that the PEG-fusion-resistant cells might be induced to fuse more extensively at higher concentrations of PEG (51). At 50% PEG, F_{16} and F_{24} cells fuse much less well than LM. However, when the concentration of PEG treatment is raised from 50% to 55%, the percentage of cells which fuses rises from 42% to 83% in the F_{16} line, and from 24% to 81% in F_{24} cells, almost to the level observed with LM cells. Light micrographs of LM cells treated with 30%, 40%, 50%, and 55% PEG, and of F_{24} cells treated with 50% and 55% PEG, and control cultures of both lines are shown in the lefthand panels of Fig. 2.

Distribution of Intramembrane Particles

It was shown previously that cold-induced aggregation of IMP is found in membranes of LM cells which have been treated with fusogenic concentrations of PEG (50). To assess further the perturbation of membranes induced by PEG treatment, we have studied freeze-fracture samples of both parental

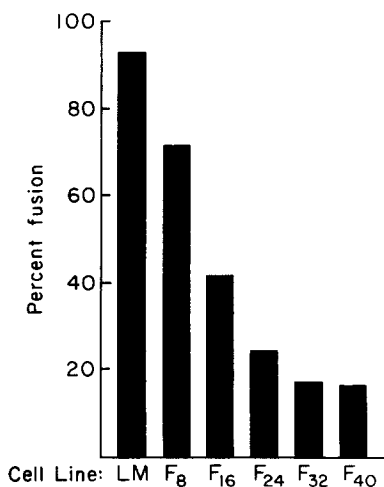


FIGURE 1 Fusion response of PEG-fusion-resistant cells. Cultures of LM (parental) cells and fusion-resistant lines selected by 8, 16, 24, 32, and 40 cycles of PEG treatment as previously described (51) were used as indicated. Confluent monolayers of cells were treated with a 50% solution of PEG and scored for fusion as described in Materials and Methods.

(LM) and fusion-resistant cells after treatment with several concentrations of PEG. In all cases presented in this paper, freeze-fracture preparations were of fixed samples which were cooled briefly to 4°C prior to fixation. Uncooled samples exhibit no IMP aggregation (50). These results are not due to artifactual perturbation during fixation, as the same patterns of aggregation were found in samples frozen without prior fixation (not shown).

The righthand panels of Fig. 2 reproduce portions of freeze-fracture electron micrographs from PEG-treated samples of LM and F_{24} cells. Each paired fracture and light micrograph are of the same cell line and PEG treatment. Treatments of F_{16} cells are not presented in this figure, but were always similar to those of F_{24} or intermediate between that of LM and that of F_{24} , as shown quantitatively in Figs. 3 and 4. Control samples (Fig. 2, B and L) show seemingly random distribution of IMP. In addition, no aggregation is visible to the eye in samples that exhibit sub-maximal fusion in the adjacent light micrographs. LM cells at 30% and 40% PEG (Fig. 2, D and F) show no apparent aggregation, although fusion is evident following 40% PEG treatment (Fig. 2 E). Similarly, F_{24} cells treated with 50% PEG show only moderate fusion (Fig. 2 M) and no aggregation of their IMP (Fig. 2 N). By contrast, 50% treatments of LM cells results in extensive cell fusion (Fig. 2 G) and dramatic aggregation of IMP (Fig. 2 H). At 55% PEG, fusion and IMP aggregation are seen in both LM cells (Fig. 2, I and J) and F_{24} (Fig. 2, O and P). Thus aggregation of IMPs is seen to occur in association with extensive cell fusion, but no aggregation is visible in incompletely fused samples.

Statistical Analysis

Visual estimation of particle distributions in a plane, assuming the random distribution as a null hypothesis, is a notoriously poor technique, subject to peculiar quirks of perception as yet incompletely understood (27). To obtain more accurate data on IMP aggregation we have adapted a simple, sensitive, quantitative assay for the analysis of particle distribution, using the V statistic (as described in Materials and Methods).

Fig. 4 shows calculations of IMP distribution (V) for each cell line and PEG treatment. For all control samples combined, the average V for the number of IMP per quadrant equals 1.05. This demonstrates that control cultures exhibit statistically random distribution: $V = 1$, shown by the dashed line in Fig. 4. In contrast, the average V in analyses of freeze-fractured LM cells treated with 50% PEG (which show a fusion index of 90%) was 2.95, indicating strong aggregation of IMP and confirming visual analysis. LM cell treated with 30% PEG (which exhibit no fusion) showed no significant deviation from control cultures ($V = 0.67$). However, treatment of LM cells with 40% PEG (resulting in 40–50% fusion) produced intermediate displays of IMP aggregation ($V = 1.62$). This low level of aggregation is statistically significant at the 1% level, but is not readily observable by eye (Fig. 3 F). Treatment of LM cells with 55% PEG results in extensive fusion and IMP aggregation ($V = 2.90$).

When fusion-deficient lines were analyzed for IMP distribution following treatment with 50% PEG (which produced much less fusion than when LM cells were similarly treated) average V's of 1.13 and 1.10 (not significantly different from 1) were recorded for F_{16} and F_{24} . We have also analyzed IMP

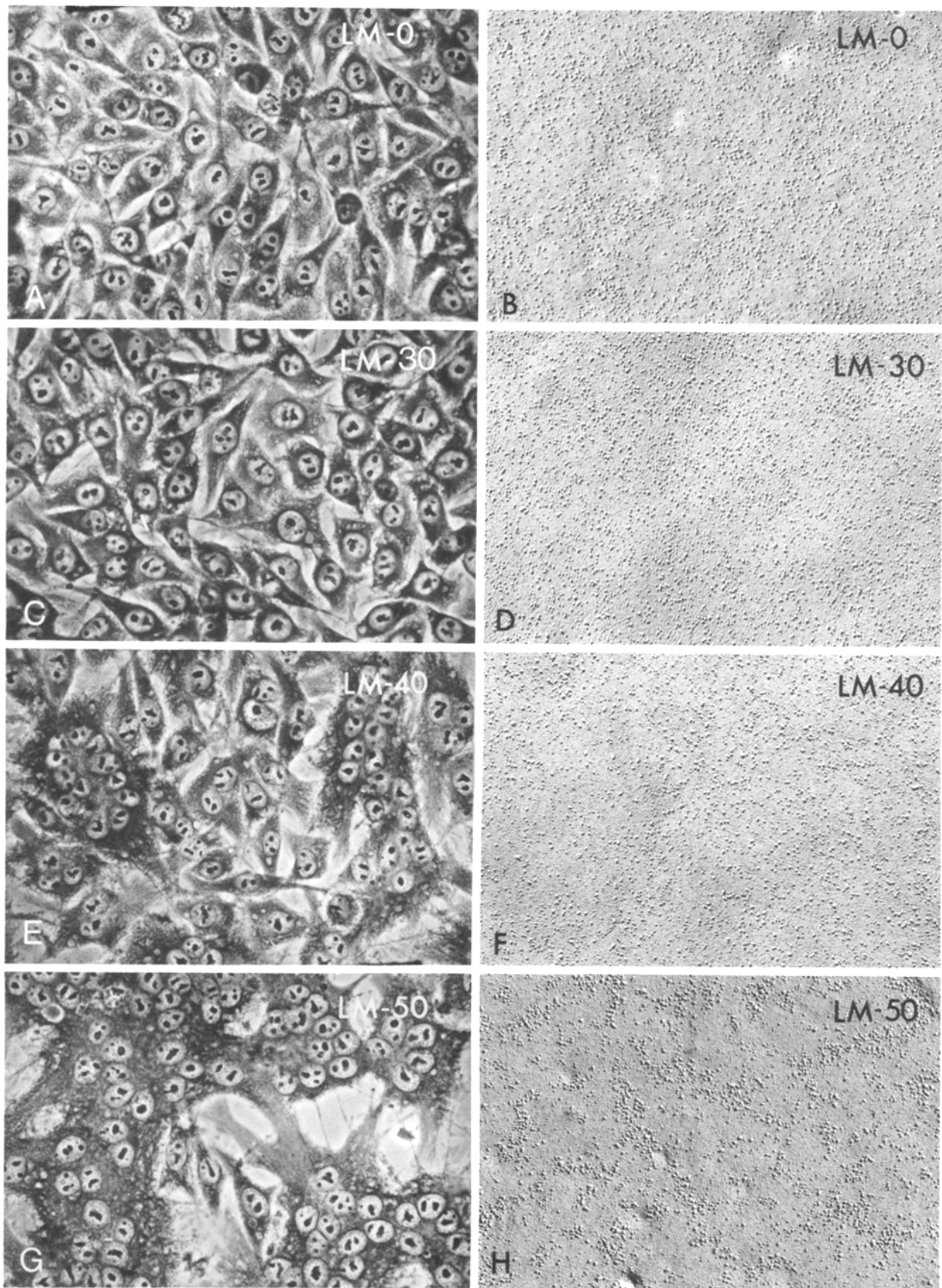
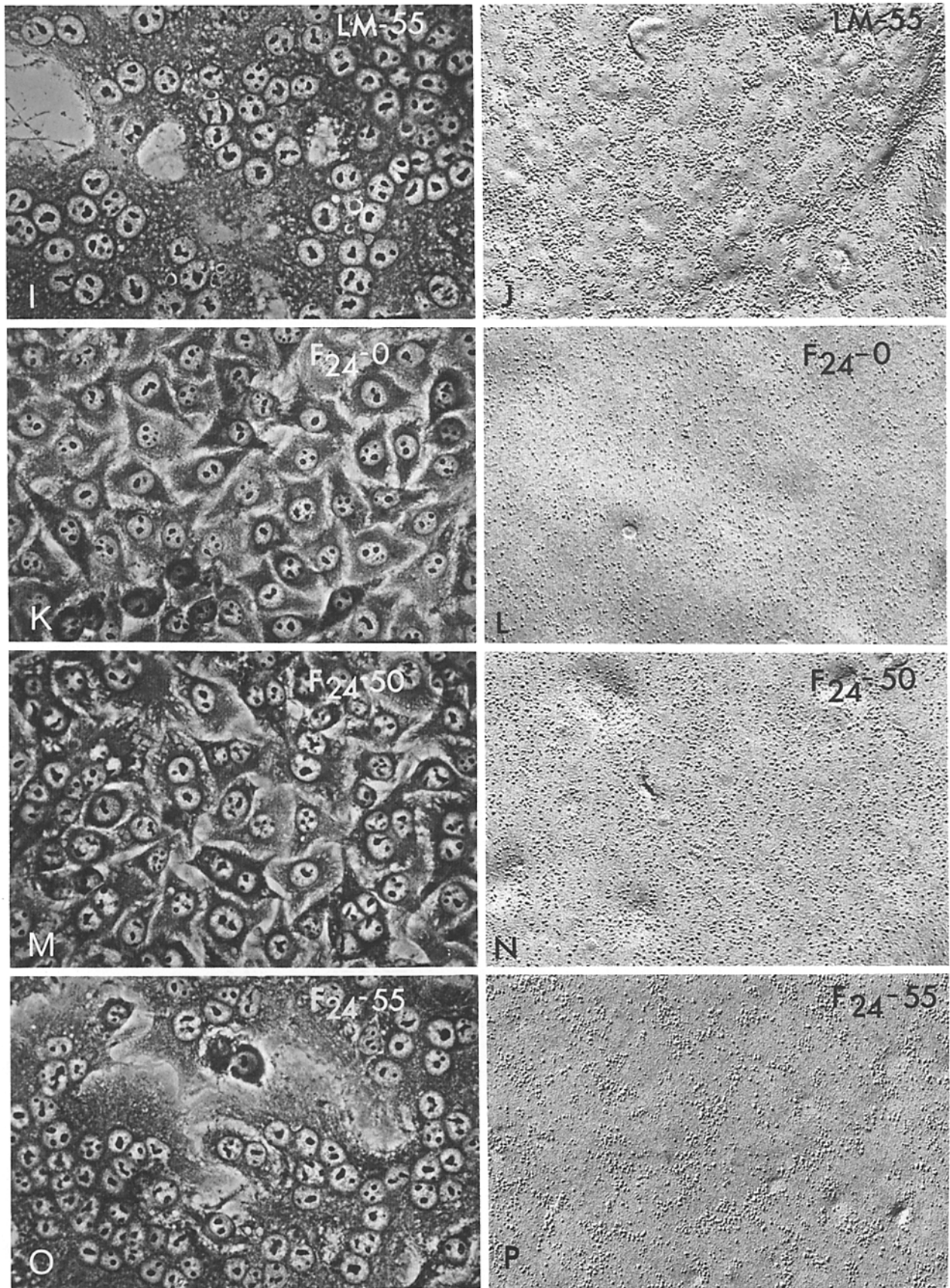


FIGURE 2 Fusion and IMP aggregation in LM (A-J) and F_{24} (K-P) cell cultures after treatment with various concentrations of PEG. Cell line and concentration of PEG are indicated in the upper right hand corner of each micrograph. (A and B) Control cultures of LM cells. (C and D) Treatment of LM cells with 30% PEG, causing neither cell fusion nor redistribution of IMP. (E and F) Treatment of LM cells with 40% PEG. Substantial fusion of cells is visible, but no aggregation of IMP can be detected by eye. (G



and *H*) 50% PEG treatment of LM cells results in pronounced cell fusion and aggregation of IMP. (*I* and *J*) LM cells treated with 55% PEG. (*K* and *L*) Control cultures of F_{24} cells. (*M* and *N*) Treatment of F_{24} cells with 50% PEG. Little fusion is seen compared with the same treatment of LM cells (*C*). (*O* and *P*) 55% PEG treatment of F_{24} cells produces extensive cell fusion and aggregation of IMP. Left side: light micrographs, $\times 850$. Right side: electron micrographs, $\times 38,000$.

distributions in F_{40} cells treated with 50% PEG and measured V as 1.21 (data not shown). Thus fusion-deficient cells (F_{16} , F_{24} , and F_{40}) exhibit no quantifiable aggregation when treated with 50% PEG, even though F_{16} cells show 42% fusion under these conditions (see Fig. 3). When the concentration of PEG was raised to 55%, however, the fusion-deficient lines studied showed extensive aggregation: $V = 3.96$ and 3.07 for F_{16} and F_{24} cells, respectively. These conditions also induced extensive

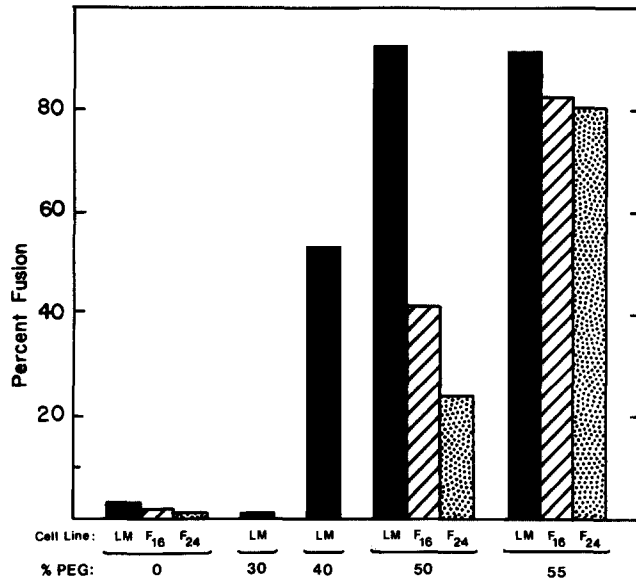


FIGURE 3 Fusion PEG of resistant lines by increased PEG concentrations. Cells were treated with various concentrations of PEG, and the results scored as in Fig. 1.

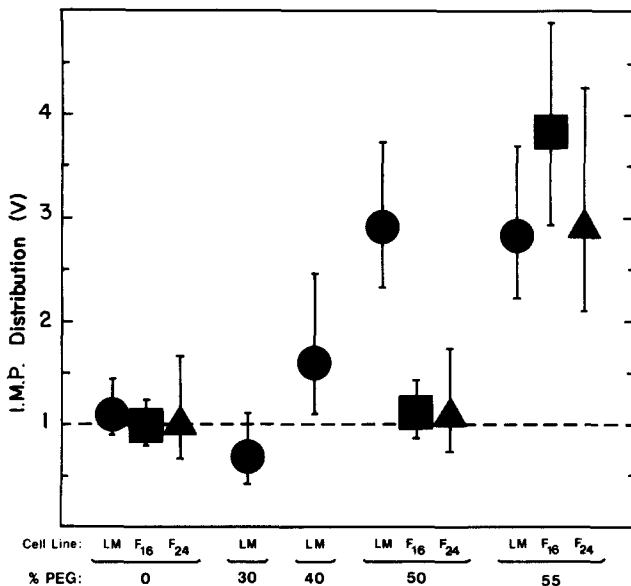


FIGURE 4 Statistical analysis of IMP aggregation in PEG treated cells. Cells were treated with various concentrations of PEG and prepared for freeze-fracture electron microscopy. Randomly chosen fields were analyzed for redistribution of IMPs as described in Materials and Methods. Error bars are 99% confidence limits calculated by the jackknife technique (54). Aggregation is extensive in heavily fused samples (LM cells treated with 50% PEG, all cultures at 55% PEG; compare with Fig. 3). Significant aggregation is also detected by statistical techniques in LM cells treated with 40% PEG, where fusion is not extensive. Note that no aggregation is found in incompletely fused PEG-resistant cells.

fusion in all these lines, as shown above. As visual analysis indicated, it appears that IMP aggregation is related to fusion in this system, but the nature of this relationship is unclear. We have tentatively identified low levels of IMP redistribution following treatment of LM cells with 40% PEG, but no IMP aggregation in F_{16} cells treated with 50% PEG, although similar levels of fusion are observed in these two samples.

Differences in the average value of V in duplicate experiments were, in general, relatively small, justifying the consideration of duplicate experiments together. In five experiments in which LM cultures were treated with 50% PEG, the average values of V were measured as 2.05, 4.71, 3.03, 2.42, and 2.33. Three trials with F_{16} cells under identical conditions yielded measurements of $V = 1.11$, 1.24, and 0.98. Paired analysis of all replicative experiments using Snedcor's F-distribution test (55) shows no statistical difference from one trial to another, but confirms differences between treatments and cell lines, as discussed above.

As an additional index of IMP distribution, we also studied the extent of aggregation by comparison with Poisson expectations. This approach has often been used by other investigators (1, 36, 43). Table I shows the results of Chi-square analysis based on differences between Poisson expectations and the observed number of IMP per quadrat. In 9 out of 10 treatments where fusion proceeded extensively, the aggregation of IMP was judged as highly significant by this technique ($P < 0.001$ in 8, $P < 0.01$ in 1, and $P < 0.1$ in 1). None of the controls or incompletely fused samples showed IMP distributions sufficiently unusual to exclude the null hypothesis of randomly distributed particles. These results generally agree with those using the V statistic, and confirm the correlation of fusion and aggregation. However, this approach fails to show aggregation in LM cells following 40% PEG treatment, in contrast to the analysis of V presented above.

DISCUSSION

IMP Aggregation and Cell Fusion

We have used the distribution of IMP as a probe for studying membrane structural changes associated with PEG-induced cell fusion. The series of cell lines resistant to fusion by PEG provides a convenient system for testing the correlation we previously observed (50) between fusion and particle aggregation. Examination of Fig. 2 shows a strong positive correlation: cold-induced aggregation of IMP occurs only where fusion is extensive, and all heavily fused samples exhibit strong aggregation. Although the nature of the freeze-fracture technique precludes determination of fusion in the individual cells whose IMP morphology was studied, two observations indicate that perturbations of IMP structure occurs in all cells of a given culture, regardless of whether they are actually involved in intercellular fusion. No significant variation in IMP distribution was detected (by jackknife analysis) between individual cells within each sample group, even though we know from light microscopic observation that each sample contains a mixture of fused and unfused cells. Secondly, IMP aggregation was still seen in sparse cultures treated with fusogenic concentrations of PEG, although these samples were, because of their low density, unable to fuse (data not shown).

The correlation between fusion and IMP aggregation indicated by visual inspection of freeze-fracture samples appears clear, but statistical analysis indicates that there are excep-

TABLE I
Comparison of Number of IMPs/Quadrat with Poisson Expectations

Cell line	Treatment	No. of quadrats	Mean	Variance (s^2)	χ^2	Degrees of freedom	P	Aggregation	
LM	Control	50	10.8	9.1	9.5	12	>0.75	-	
		60	11.3	17.2	18.0	13	>0.1	-	
		80	12.9	14.7	19.7	15	>0.1	-	
	30% PEG	40	12.9	12.1	13.2	13	>0.25	-	
		40% PEG	50	12.9	22.5	12.2	14	>0.5	-
		50% PEG	60	10.1	26.7	56.6	12	<0.001	+
			60	10.7	40.0	95.5	13	<0.001	+
	55% PEG	70	9.4	21.3	21.2	13	<0.1	+/-	
		70	9.7	25.5	44.4	12	<0.001	+	
		70	10.3	67.8	99.6	13	<0.001	+	
		55% PEG	50	11.3	31.2	28.9	13	<0.01	+
90			13.3	39.7	182.7	15	<0.001	+	
F ₁₆	Control	50	8.8	11.1	14.0	11	>0.1	-	
		50	9.9	9.5	9.1	12	>0.75	-	
		60	10.0	11.0	10.4	12	>0.5	-	
	50% PEG	50	12.5	18.5	9.3	13	>0.5	-	
		50	10.0	12.7	10.3	12	>0.5	-	
		60	9.7	12.4	11.2	12	>0.5	-	
	55% PEG	90	10.9	47.4	111.5	14	<0.001	+	
		90	12.8	51.3	167.2	15	<0.001	+	
F ₂₄	Control	40	10.7	11.9	6.9	11	>0.75	-	
	50% PEG	50	9.4	15.0	10.4	11	>0.25	-	
	55% PEG	70	9.9	30.8	37.8	12	<0.001	+	

tions. Comparison of Figs. 3 and 4 shows that treatments of PEG-resistant cells with concentrations of PEG which induce low levels of fusion produced no alteration of particle distribution in the membrane. Treatment of F₁₆ cells with 50% PEG resulted in no measurable aggregation of IMP even though 42% of all cells fused. In contrast, when comparable levels of fusion were induced in LM cells by treatment with 40% PEG, intermediate levels of IMP aggregation were observed. This apparent discrepancy observed with LM and F₁₆ cells suggests a differential effect of PEG on aggregation and fusion.

Mechanisms for membrane fusion in mammalian cells have been proposed involving either specific interactions between particle-rich areas (9, 52), or nonspecific lipid-lipid interaction between particle-free areas in closely apposed cells (2, 5, 10, 33, 40, 57). Interactions between membrane components must certainly be important in the formation of fusion bridges. However, in the PEG fusion system, our data suggest at least partial independence of PEG-induced fusion and IMP aggregation and raise the possibility that aggregation is not absolutely required for fusion.

One effect of PEG and other fusogens may be to alter membrane structure in such a way as to induce both fusion and to reveal, in cooled samples, IMP aggregation. Thus, both fusion and aggregation could reflect another membrane alteration and not be causally related to each other. This other alteration could occur either directly, through the interaction of PEG with membrane proteins or lipids, or indirectly by PEG-induced changes in such factors as pH or effective hydration of the membrane. The possibility also exists that PEG treatment exerts its effect through changes in membrane fluidity. The physical state of membrane lipids with respect to the fluid transition temperature is known to affect clustering and dispersion of integral membrane proteins and IMP (4, 59). In addition to interactions of PEG with membrane

components at the molecular level, larger-scale effects of PEG may be of importance in the fusion process. PEG is known to alter the shedding of membrane surface components in some cells (35), although the blistered appearance usually associated with such shedding is not found in the LM line.

Statistical Analysis of Particle Distributions

In approaching quantitative analysis of IMP distribution in other systems, some investigators have sought to compare fracture faces visually with arbitrarily assigned (19) or computer-generated (20, 21) standards of increasing aggregation. Others have determined either the density (6) or the extent (53) of areas that appear most aggregated to the eye. Although visual analysis of IMP distribution can distinguish extensive aggregation or order, its sensitivity is inadequate when distributional differences are subtle. Consequently, mathematical analysis is necessary for detailed comparison of IMP distribution in fractured membranes.

Several types of measurements have been applied to the analysis of particle distributions in membranes. Techniques of radial distribution analysis (18, 34, 45) allow accurate modelling of IMP aggregation in one or a few micrographs (22, 36, 43). These techniques involve the selection of a representative micrograph and calculation of relative frequencies over a range of interparticle distances. In many experiments, cell-to-cell variation within a sample necessitates analyzing several micrographs in each sample. To do so with the detail of these techniques is prohibitively time-consuming and expensive. Perhaps the most frequently used approach to particle distribution analysis (1, 36, 45) involves generating frequencies of particle densities in randomly chosen quadrats and comparing these frequencies with Poisson expectations by Chi-square analysis (Table I). This technique is difficult to apply to large numbers of samples, and its sensitivity is

severely compromised when particle densities vary from micrograph to micrograph. In addition, it is subject to the assumptions of Poisson distribution implicit in the Chi-square model.

The V statistic provides a useful method for comparing IMP densities, as shown above. The presence of \bar{x} in the denominator corrects for differences in average particle density, allowing direct comparison between different cells. One particularly useful aspect of the V statistic is that it allows distinctions to be made not only between randomly and nonrandomly distributed samples, but between two different forms of nonrandom patterns: aggregation and order. Aggregation, such as the clustering of IMP studied in this report, is reflected in values of $V > 1$, while ordered samples (the regular arrangement of IMP into hexameric groups, for example) result in abnormally even distribution of IMP between quadrats and values of $V < 1$. In the extreme case where all particles are fixed in a rigid lattice, V equals zero. Measurement of V allows relatively rapid quantification of many micrographs, achieving its sensitivity through the analysis of a few quadrats in each of many samples, rather than extensive analysis of a single sample. As the error bars in Fig. 4 indicate, this sensitivity is considerable, allowing discrimination between samples at levels far below that which can be distinguished by eye.

The analysis of spatial distributions is a problem with wide applicability in many fields, including ecology (23), astrophysics (44), and epidemiology (47), as well as biology. Further characterization and discussion of the V statistic and its application will be presented elsewhere (D. S. Roos, D. S. Pearson, and B. Singer, manuscript in preparation).

Fusion-resistant Cell Lines

The availability of cells resistant to PEG-induced fusion provides a particularly useful system for the characterization of cell fusion. It is interesting, however, that the gradual selection for isolation of these cells does not lead to the production of a completely unfusible cell line (Fig. 1). Our most PEG-resistant cells still show ~15–20% fusion, more than five times background levels. The fact that these cells still remain susceptible to the fusogen may indicate a limit to the plasticity of cell architecture below which viability is reduced. Further changes, leading to even greater fusion resistance, may kill the cell. Selection thus may reach its limit at the threshold of cellular adaptability.

The extremely lengthy selection required to obtain these cells points to the complexity of their genetic makeup with respect to the fusion process (51). F_{32} cells are the product of greater than 10^{12} -fold selection (calculated from the number of survivors after each cycle of PEG treatment) from an initial population of 4×10^6 cells. Analysis of biochemical and behavioral differences between LM cells and their resistant daughter lines should help to clarify factors involved in cell fusion. One particularly intriguing characteristic, currently under investigation, is the observation that cell lines resistant to fusion by PEG fuse better than the parental cells when incubated with various paramyxoviruses (D. S. Roos and P. W. Choppin, unpublished data). This indicates that certain factors, relating either to conditions appropriate for fusion or the actual fusion mechanisms, differ between virus-induced and PEG-fusion.

We wish to thank Anita Oulette for excellent technical assistance. Discussion with Dr. Morris J. Karnovsky of Harvard University was

extremely helpful throughout this study. The advice of Dr. Burton Singer of Columbia University and David S. Pearson of the Kiewit Computation Center, Dartmouth College, on statistical and computational matters dealt with in this paper is gratefully acknowledged.

This work was supported by National Institute of Child Health and Human Development grants HD 04807 and HD 06276 (to R. L. Davidson) National Institute of Allergy and Infectious Diseases grant AI 17945 (to J. M. Robinson) and a National Science Foundation pre-doctoral fellowship award to D. S. Roos.

Received for publication 4 April 1983, and in revised form 6 June 1983.

REFERENCES

1. Abbas, A. K., K. A. Ault, M. J. Karnovsky, and E. R. Unanue. 1975. Non-random distribution of surface immunoglobulin on murine B lymphocytes. *J. Immunol.* 114:1197–1204.
2. Ahkong, Q. F., D. Fisher, W. Tampion, and J. A. Lucy. 1975. Mechanisms of cell fusion. *Nature (Lond.)* 253:194–196.
3. Allen, T. M., L. McAllister, S. Mausolf, and E. Gyorffy. 1981. Liposome-cell interactions. A study of the interactions of liposomes containing entrapped anti-cancer drugs with the EMT6, S49 and AE1 (transport-deficient) cell lines. *Biochim. Biophys. Acta.* 643:346–362.
4. Armond, P. A., and L. A. Staehelin. 1979. Lateral and vertical displacement of integral membrane proteins during lipid phase transition in *Anacystis nidulans*. *Proc. Natl. Acad. Sci. USA* 76:1901–1905.
5. Asano, A., and K. Sekiguchi. 1978. Redistribution of IMPs in human erythrocytes induced by HVJ (Sendai virus): a prerequisite for the virus-induced cell fusion. *J. Supramol. Struct.* 9:441–452.
6. Baudhuin, P., M.-A. Leroy-Houyet, J. Quintart, and P. Berthet. 1975. Application of cluster analysis for characterization of spatial distribution of particles by stereological methods. *J. Microsc. (Oxf.)* 115:1–17.
7. Blow, A. M. J., G. M. Botton, D. Fisher, A. H. Goodall, C. P. S. Tilcock, and J. A. Lucy. 1978. Water and calcium ions in cell fusion induced by PEG. *FEBS (Fed. Eur. Biochem. Soc.) Lett.* 94:305–310.
8. Branton, D., S. Bullivant, N. B. Gilula, M. J. Karnovsky, H. Moor, K. Muhlenhaler, D. H. Northcote, L. Packer, B. Satir, P. Satir, V. Speth, L. A. Staehelin, R. L. Steere, and R. S. Weinstein. 1975. Freeze etching nomenclature. *Science (Wash. D.C.)* 190:54–56.
9. Burwen, S. J., and B. H. Satir. 1977. A freeze-fracture study of early membrane events during mast cell secretion. *J. Cell Biol.* 73:660–671.
10. Chi, E. Y., D. Lagunoff, and J. K. Koehler. 1976. Freeze-fracture study of mast cell secretion. *Proc. Natl. Acad. Sci. USA* 73:2823–2827.
11. Dahl, G., C. Schudt, and M. Gratzl. 1978. Fusion of isolated myoblast plasma membranes. An approach to the mechanism. *Biochim. Biophys. Acta.* 514:105–116.
12. Davidson, R. L. 1977. Genetics of cultured mammalian cells, as studied by somatic cell hybridization. *Natl. Cancer Inst. Monograph No. 48.* 21–30.
13. Davidson, R. L., and P. S. Gerald. 1977. Improved techniques for the induction of mammalian cell hybridization by polyethylene glycol. *Somatic Cell Genet.* 2:165–176.
14. Davidson, R. L., and P. S. Gerald. 1977. Induction of mammalian somatic cell hybridization by polyethylene glycol. *Methods Cell Biol.* 15:325–338.
15. Davidson, R. L., K. A. O'Malley, and T. B. Wheeler. 1976. Polyethylene glycol-induced mammalian cell hybridization: effect of polyethylene glycol molecular weight and concentration. *Somatic Cell Genet.* 2:271–280.
16. de Laat, S. W., L. G. J. Tertoolen, and J. G. Bluemink. 1981. Quantitative analysis of the numerical and lateral distribution of intramembrane particles in freeze-fractures of biological membranes. *Eur. J. Cell Biol.* 23:273–279.
17. de St. Groth, S. F., and D. Scheidegger. 1980. Production of monoclonal antibodies: strategy and tactics. *J. Immunol. Methods.* 35:1–21.
18. Diggle, P. J., J. Besag, and J. T. Gleaves. 1976. Statistical analysis of spatial point patterns by means of distance methods. *Biometrics.* 32:659–667.
19. Elgsaeter, A., and D. Branton. 1974. Intramembrane particle aggregation in erythrocyte ghosts. I. The effects of protein removal. *J. Cell Biol.* 63:1018–1030.
20. Finegold, L. 1976. Cell membrane fluidity: molecular modeling of particle aggregation seen in electron microscopy. *Biochim. Biophys. Acta.* 448:393–398.
21. Finegold, L. 1979. Mobility in membranes in two dimensions. In *Physical Chemical Aspects of Cell Surface Events in Cellular Recognition*. C. DeLisi and R. Blumenthal, editors. Elsevier/North-Holland, Amsterdam. 129–146.
22. Gershon, N. D., A. Dempsey, and C. W. Stackpole. 1979. Analysis of local order in the spatial distribution of cell surface molecular assemblies. *Exp. Cell Res.* 122:115–126.
23. Grieg-Smith, P. 1964. *Quantitative Plant Ecology*. 2nd edition. Butterworth Press, London.
24. Harris, H., and J. F. Watkins. 1965. Hybrid cells derived from mouse and man—artificial heterokaryons of mammalian cells from different species. *Nature (Lond.)* 205:640–646.
25. Harter, D. H., and P. W. Choppin. 1967. Cell-fusing activity of visna virus particles. *Virology.* 31:279–288.
26. Holmes, K. V., and P. W. Choppin. 1966. On the role of the response of the cell membrane in determining virus virulence. Contrasting effects of the parainfluenza virus SV5 in two cell types. *J. Exp. Med.* 124:501–520.
27. Julesz, B. 1981. Textons, the elements of texture perception and their interactions. *Nature (Lond.)* 290:91–97.
28. Kao, K. N., and M. R. Michayluk. 1974. A method for high-frequency intergeneric fusion of plant protoplasts. *Planta (Berl.)* 115:355–367.
29. Kim, J., and Y. Okada. 1981. Morphological changes in Ehrlich ascites tumor cells during the cell fusion reaction with HVJ (Sendai virus). II. Cluster formation of IMPs in the early stage of cell fusion. *Exp. Cell Res.* 132:125–136.
30. Klebe, M. J., and M. G. Mancuso. 1981. Chemicals which promote cell hybridization. *Somatic Cell Genet.* 7:473–488.
31. Knutton, S. 1979. Studies on membrane fusion III. Fusion of erythrocytes with polyethylene glycol. *J. Cell Sci.* 36:61–72.
32. Knutton, S., and T. Bachi. 1980. The role of cell swelling and haemolysis in Sendai-

- virus induced cell fusion and in the diffusion of incorporated viral antigens. *J. Cell Sci.* 42:153-167.
33. Lawson, D., M. C. Raff, B. Gomperts, C. Fewtrell, and N. B. Gilula. 1977. Molecular events during membrane fusion. A study of exocytosis in rat peritoneal mast cells. *J. Cell Biol.* 72:242-259.
 34. Markovics, J., L. Glass, and G. G. Maul. 1974. Pore patterns on nuclear membranes. *Exp. Cell Res.* 85:443-451.
 35. McCammon, J. R., and V. S. C. Fan. 1979. Release of membrane constituents following polyethylene glycol treatment of HEp-2 cells. *Biochim. Biophys. Acta.* 551:67-73.
 36. Mehlhorn, R. J., and L. Packer. 1976. Analysis of freeze-fracture electron micrographs by a computer based technique. *Biophys. J.* 16:613-625.
 37. Miller, R. G. 1974. The jackknife—a review. *Biometrika.* 61:1-15.
 38. Mosteller, F., and J. W. Tukey. 1968. Data analysis, including statistics. In *The Handbook of Social Physiology*. Volume II, 2nd edition. G. Lindsey and E. Aronson, editors. Addison-Wesley Publishing Co., Reading, MA.
 39. Okada, Y. 1962. Analysis of giant polynuclear cell formation caused by HVJ virus from Ehrlich's ascites tumor cells. I. Microscopic observation of giant polynuclear cell formation. *Exp. Cell Res.* 26:98-107.
 40. Orci, L., A. Perrelet, and D. S. Friend. 1977. Freeze-fracture of membrane fusions during exocytosis in pancreatic B-cells. *J. Cell Biol.* 75:23-30.
 41. Papahadjopoulos, D., editor. 1977. *Liposomes and Their Uses in Biology and Medicine*. Ann. N.Y. Acad. Sci. Vol. 308.
 42. Papahadjopoulos, D., G. Poste, and W. J. Vail. 1979. Studies on membrane fusion with natural and model membranes. *Methods Cell Biol.* 19:1-121.
 43. Pearson, R. P., S. W. Hui, and T. P. Stewart. 1979. Correlative statistical analysis and computer modeling of intramembranous particle distributions in human erythrocyte membranes. *Biochim. Biophys. Acta.* 557:265-282.
 44. Peebles, P. J. E. 1973. Statistical analysis of catalogs of extragalactic objects 1. *Theor. Astrophys. J.* 185:413-440.
 45. Perelson, A. S. 1978. Spatial distribution of surface immunoglobulin on B lymphocytes. *Exp. Cell Res.* 112:309-321.
 46. Pfeiffer, J. R., J. M. Oliver, and R. D. Berlin. 1980. Topographical distribution of coated pits. *Nature (Lond.)* 286:727-729.
 47. Pike, M. C., and P. G. Smith. 1968. Disease clustering: a generalization of Knox's approach to the detection of space-time interactions. *Biometrics.* 24:541-556.
 48. Poste, G., and G. L. Nicholson, editors. 1978. *Membrane Fusion*. *Cell Surf. Rev.* Vol. 5.
 49. Pontecorvo, G. 1975. Production of mammalian somatic cell hybrids by means of polyethylene glycol treatment. *Somatic Cell Genet.* 1:397-400.
 50. Robinson, J. M., D. S. Roos, R. L. Davidson, and M. J. Karnovsky. 1979. Membrane alterations and other morphological features associated with polyethylene glycol-induced cell fusion. *J. Cell Sci.* 40:63-75.
 51. Roos, D. S., and R. L. Davidson. 1980. Isolation of mouse cell lines resistant to the fusion-inducing effect of polyethylene glycol. *Somatic Cell Genet.* 6:381-390.
 52. Schudt, C., G. Dahl, and M. Gratzl. 1976. Calcium-induced fusion of plasma membranes isolated from myoblasts grown in culture. *Cytobiologie.* 13:211-223.
 53. Shotton, D., K. Thompson, L. Wofsy, and D. Branton. 1978. Appearance and distribution of surface proteins of the human erythrocyte membrane. An electron microscope and immunochemical labelling study. *J. Cell Biol.* 76:512-531.
 54. Singer, B. S., R. Sager, and Z. Ramanis. 1976. Chloroplast genetics of *Chlamydomonas* III. Closing the circle. *Genetics.* 83:341-354.
 55. Snedecor, G. W., and W. G. Cochran. 1967. *Statistical Methods*. 6th edition. Iowa State, Ames, IA.
 56. Tavassoli, M., N. S. Kosower, C. Halverson, M. Aoki, and E. M. Kosower. 1980. Membrane fusion induced by the membrane mobility agent A₇C. *Biochim. Biophys. Acta.* 601:544-558.
 57. Volsky, D. J., and A. Loyter. 1978. Inhibition of membrane fusion by suppression of lateral movement of membrane proteins. *Biochim. Biophys. Acta.* 514:213-224.
 58. Vos, J., Q. F. Ahkong, G. M. Botham, S. J. Quirk, and J. A. Lucy. 1976. Changes in the distribution of intramembrane particles in hen erythrocytes during cell fusion induced by the bivalent-cation ionophore A23187. *Biochem. J.* 158:651-653.
 59. Wallace, B. A., and D. M. Engelman. 1978. The planar distribution of surface proteins and intramembrane particles in *Acoelasma laidlawii* are differently affected by the physical state of the membrane lipids. *Biochim. Biophys. Acta.* 508:431-449.
 60. Wang, E. W., D. S. Roos, M. H. Heggeness, and P. W. Choppin. 1982. Function of cytoplasmic fibers in syncytia. *Cold Spring Harbor Symp. Quant. Biol.* 46:997-1012.
 61. Weinstein, R. S. 1976. Changes in plasma membrane structure associated with malignant transformation in human urinary bladder epithelium. *Cancer Res.* 36:2518-2524.
 62. Yee, A. G., G. D. Fischbach, and M. J. Karnovsky. 1978. Clusters of intramembranous particles on cultured myoblasts at sites that are highly sensitive to acetylcholine. *Proc. Natl. Acad. Sci. USA* 75:3004-3008.